European Journal of Pharmaceutical Sciences 156 (2021) 105587

Contents lists available at ScienceDirect

European Journal of Pharmaceutical Sciences

journal homepage: www.elsevier.com/locate/ejps

Androstano-arylpyrimidines: Novel small molecule inhibitors of MDR1 for sensitizing multidrug-resistant breast cancer cells

Mohana Krishna Gopisetty[a], Dóra Izabella Adamecz[a], Ferenc István Nagy[a], Ádám Baji[b], Vasiliki Lathira[c], Márton Richárd Szabó[d], Renáta Gáspár[d], Tamás Csont[d], Éva Frank[b], Mónika Kiricsi[a,*]

[a] Department of Biochemistry and Molecular Biology, Doctoral School of Biology, University of Szeged, Közép fasor 52, H-6726, Szeged, Hungary
[b] Department of Organic Chemistry, University of Szeged, Dóm tér 8., Szeged H-6720, Hungary
[c] School of Biology, Faculty of Sciences, Aristotle University of Thessaloniki, University Campus, Thessaloniki 54124, Greece
[d] Metabolic Diseases and Cell Signaling (MEDICS) Research Group, Institute of Biochemistry, Interdisciplinary Center of Excellence, University of Szeged, Dóm tér 9., Szeged H-6720, Hungary

ARTICLE INFO

Keywords:
Multidrug resistance
Inhibition of multidrug resistance protein 1
Androstano-arylpyrimidines
Endoplasmic reticulum stress
Breast cancer

ABSTRACT

Apart from the numerous physiological functions of MDR1, it is widely known for its role in granting multidrug resistance to cancer cells. This ATP-driven transmembrane protein exports a wide range of chemotherapeutic agents from cancer cells, thereby deterring drugs to reach effective intracellular concentrations. Thus, inhibition of MDR1 expression or function would be a viable option to enhance the accumulation of cytotoxic agents in cancer cells which in turn could improve significantly the success rate of chemotherapy. Although, several pharmacological inhibitors have been designed and tested in the past, due to their unsuccessful translation to clinical application, there is still ongoing research to find suitable compounds to manipulate MDR1 function and potentially overturn multidrug resistance.

In the present study, we demonstrate that novel DHT-derived A-ring-fused arylpyrimidinone derivatives, based on their acetylation status, can inhibit MDR1 efflux activity in MDR1 overexpressing multidrug-resistant breast adenocarcinoma cells. Strikingly, all derivatives carrying an acetoxy group on the sterane D-ring were highly potent in hindering Rhodamine 123 export via MDR1, however deacetylated molecules were not capable to exert a similar effect on multidrug resistant cancer cells. The possible molecular and cellular mechanisms underlying the efflux pump inhibiting function of acetylated derivatives were dissected using the most potent MDR1 inhibitor, compound **10g** and its deacetylated counterpart (**11g**). Importantly, molecule **10g** was able to sensitize drug resistant cells to doxorubicin-induced apoptosis, further verifying the highly advantageous nature of efflux pump inhibition upon chemotherapy. Our experiments also revealed that neither mitochondrial damage, nor *MDR1* gene regulation could lay behind the MDR1 inhibitory function of compound **10g**. Molecular docking studies were carried out to analyze the interactions of **10g** and **11g** with MDR1, however no significant differences in their binding properties were observed. Nevertheless, our results indicate that the ER stress inducing potential of molecule **10g** might be the fundamental mechanism behind its inhibitory action on MDR1. With additional studies, our work can yield a structural platform for a new generation of small molecule MDR1 inhibitors to sensitize drug resistant cancer cells and at the same time it elucidates the exemplary involvement of endoplasmic reticulum stress in the molecular events to defeat multidrug resistance.

1. Introduction

Although a considerable amount of scientific effort has been dedicated to understand the cellular and molecular events that drive cancer recurrence, invasion and metastasis, and important advancements have been achieved in identifying potential pharmacological targets, nevertheless, adequately competent therapeutic approaches to defeat malignant cells are still wanted. The first line treatment for most cancer types is usually, small molecular drug-based chemotherapy, where the development of drug resistance is, unfortunately, a likely outcome. Decreased sensitivity to several cytotoxic drugs and broad cross-resistance to a large number of structurally dissimilar antineoplastic

* Corresponding author.
E-mail address: kiricsim@bio.u-szeged.hu (M. Kiricsi).

https://doi.org/10.1016/j.ejps.2020.105587
Received 19 May 2020; Received in revised form 7 August 2020; Accepted 4 October 2020
Available online 08 October 2020

agents emerge quickly, advancing the evolution of multidrug-resistant (MDR) cancer phenotypes. MDR, either intrinsic or acquired, displays a substantial hurdle to effective cancer therapy leading to poor patient survival (Luqmani, 2005). Although the cellular and molecular features of MDR involve modification of signaling pathways, endurance of oxidative stress and increased apoptotic threshold, the major component of the cancer cells' strategy to reduce cellular accumulation and thereby evading the toxic effects of chemotherapy drugs is the overexpression of various efflux pumps. Such an ATP-dependent transmembrane drug transporter protein is P-glycoprotein, also known as MDR1 or ABCB1, which is encoded by the multidrug resistance gene 1 (*MDR1*). Via such ABC transporters - membrane-residing pumps containing ATP binding motives - cytotoxic agents can be readily expelled from the cytoplasm immediately after their uptake, at almost the same speed as they entered tumor cells, leaving no time to exert their anticancer activities (Gillet and Gottesman, 2010; Szakács et al., 2014, 2004). As a consequence, a broad spectrum of approaches was tested to suppress the expression and the function of ABC transporters, in particular, those of MDR1, in order to potentially overturn MDR (Callaghan et al., 2014; Chen and Tiwari, 2011; Choi and Yu, 2014). Along this line, based on the protein structure and on the conformational changes associated with MDR1 efflux activity, a multitude of inhibitors have been designed and developed to hinder drug transport across MDR1; sadly, translation of their application to the clinical practice have failed owing to side-effects related to their pharmacological properties (i.e. cardiotoxicity elicited by verapamil treatment) (Coley, 2010; Ekins et al., 2002; Kathawala et al., 2015; Robert and Jarry, 2003). Despite the somewhat disappointing results of the clinical trials performed with some of the selected MDR1 inhibitors, there is still intensive ongoing research to find the ultimate compound/s with the unique capability to manipulate specifically MDR1 activity without exerting unpredictable toxicities, thereby opening avenues to overcome MDR cancer.

Among the numerous candidates designed for MDR1 inhibition, several natural and synthetic steroids have already been examined (De Ravel et al., 2015). In synthetic studies, physiologically relevant steroids have been utilized as precursors, where structure optimization was aimed to establish or enhance the inhibiting performance of the molecule/s on MDR1 without triggering undesired interactions. Modulation of the substitution profile of natural sex-hormones, glucocorticoids or other steroids enables a huge versatility of chemical modifications leading to a substantial transformation of the physicochemical, biological and pharmacokinetic properties of the parent compound. In fact, progesterone and its synthetic derivatives have been thoroughly screened and it was found that the fairly weak activity of progesterone on MDR1 could be enhanced by introducing 7α-thiophenyl groups, 11α-benzoate, and carbamate substituents or via modifications at the 17β-acetyl side chain (Ichikawa-Haraguchi et al., 1993; Leonessa et al., 2002). MDR1 inhibiting properties were observed also for steroidal anti-estrogens, for some synthetic glucocorticoid derivatives, as well as for modified primary and secondary conjugated and unconjugated bile acids (Cooray et al., 2006; Lo et al., 2008; Rocheblave et al., 2016). Based on structure−activity studies, modeling and docking investigations and fluorescence-based techniques, it seems plausible that interactions between MDR1 and its steroid modulators are centered near the ATP-binding domain of the transporter, suggesting that the influence on efflux activity exhibited by these compounds is associated with the ATP-driven conformational change required for drug transport (Dayan et al., 1997; Li et al., 2005; Mares-Samano et al., 2009a).

Modifications of natural steroids by heterocycles either connected to or condensed with one of the steroid rings have gathered grounds in recent developments. Among various modifications, the introduction of pyrimidines is exceptionally relevant as the resultant hybrid derivatives with high stability, tunable composition and multifunctionality, manifest an extensive range of biological properties, such as antiviral, antimicrobial, antioxidant, as well as anti-cancer activities (Gore and Rajput, 2013; Kaur et al., 2014; Mohana Roopan and Sompalle, 2016). In view of the biological relevance of steroidal heterocycles, novel arylpyrimidine-fused androstanes were recently synthesized via three-component, modified Biginelli-type reactions under microwave irradiation and the cytotoxicity of the compounds was screened in vitro on two prostate cancer (PC-3 and DU 145), on MCF-7 breast cancer and on non-cancerous lung fibroblast (MRC-5) cell lines (Baji et al., 2017). Remarkable association between structure and biological activity were noted since acetylated, A-ring-fused 4′-arylpyrimidin-2′-one derivatives of dihydrotestosterone (DHT) 17-acetate exhibited significant cytotoxicity, whereas deacetylated analogs failed to induce cancer cell death. We concluded that arylpyrimidines can be utilized in future drug design and synthetic approaches as structural scaffolds of androstanes, motivating the rational design and pharmacological investigation of additional derivatives and the highly advantageous cytotoxic features of acetylated androstanes with the arylpyrimidine modifications could be further exploited to kill different types of cancer cells.

Thus, our next aim was to test the remarkable anticancer performance of acetylated DHT- arylpyrimidinone derivatives on cancer cells with multidrug-resistant phenotype and to examine the impact of these compounds on the efflux activity and on the cellular responses of MDR cancer cells. Therefore, the present study was undertaken with the aim to examine the MDR1 inhibiting properties of a series of semi-synthetic, acetylated as well as deacetylated A-ring-modified heterocyclic DHT derivatives - selected from the compound library synthesized and investigated previously (Baji et al., 2017) - in order to reveal structure−activity criteria relevant for attenuating drug efflux via MDR1. Since we could identify several compounds exhibiting prominent MDR1 inhibiting capacity, using one suitable compound the mechanism behind its action on multidrug-resistant breast cancer cells has been investigated in details. Since attenuation of MDR1 activity by the synthetized androstane derivatives can be the result of transcriptional and translational suppression of *MDR1*, or of mitochondrial dysfunction leading to decreased ATP generation, apoptosis or endoplasmic reticulum stress, we tested these cellular and molecular events in multidrug-resistant MCF-7/KCR cells, following treatments with the most promising DHT derivative.

2. Materials and methods

2.1. Synthesis of androstano-pyrimidinones

The synthesis of arylpyrimidinone-modified DHT derivatives was reported previously (Baji et al., 2017). Briefly, DHT-acetate (1 mmol), *para*-substituted benzaldehyde (2 mmol) and urea (1 mmol) were dissolved in acetic acid (10 mL) and concentrated H_2SO_4 (2 drops) was added. The mixture was irradiated in a closed vessel at 110 °C for 10 min using a CEM Corporation Focused Microwave System, Model Discover SP. After completion of the reaction, the mixture was poured into saturated $NaHCO_3$ solution (10 mL) and extracted with dichloromethane (2 × 10 mL). The combined organic layers were washed with water (10 mL), dried over anhydrous Na_2SO_4 and evaporated in vacuo. The residue was then dissolved in acetone (20 mL) and 1 mL Jones reagent (1.8 M) was added. The mixture was poured into water after 30 min of stirring at room temperature, and extracted with dichloromethane (2 × 10 mL). The combined organic layers were dried over anhydrous Na_2SO_4 and evaporated in vacuo. The crude product was purified by column chromatography using MeOH/CH_2Cl_2 = 5:95 as eluent to give **10b−*g*** (Yields: 60−69%). For deacetylation, compound **10b–g** (0.25 mmol) was dissolved in methanol (10 mL), and KOH (1 mmol) was added. The solution was stirred at room temperature for 8 h, and then diluted with water. After adding NH_4Cl, the mixture was cooled and the resulting precipitate was filtered off, washed with water and dried to give **11b−*g*** (Yield: 85−95%). The original compound numbers used in Baji et al. (Baji et al., 2017) were retained in this manuscript for clarity and comparability.

2.2. Cell culture

The MCF-7 human breast adenocarcinoma cell line was obtained from ATCC. The drug-resistant MCF-7/KCR cell line was developed from MCF-7 under selection pressure using doxorubicin from 10 nM to 1 μM concentration (Kars et al., 2006). Cell lines were maintained in RPMI-1640 medium (LONZA) supplemented with 10% FBS, 2 mM glutamine and penicillin-streptomycin solution at 37 °C, 5% CO_2 and 95% humidity. MCF-7/KCR cells were cultured in media with 1 μM doxorubicin for 1 week then in culture medium without doxorubicin for 1 week to maintain the drug-resistant phenotype. Before experiments, MCF-7/KCR cells were grown in a doxorubicin-free medium.

2.3. Rhodamine 123 accumulation assay

MCF-7/KCR cells in 2 × 10^6 cells/well density were treated with either 20 μM of compound **10b, 10c, 10d, 10f, 10g** or **11b, 11c, 11d, 11f, 11g** for 24 h or with verapamil in 40 μM concentration for 2 h. Then cells were washed and re-suspended in serum-free RPMI-1640 medium containing 10 μM of Rhodamine 123 (RH123, Sigma-Aldrich). Following 2 h incubation, cells were washed and RH123 fluorescence of at least 10,000 cells/sample was measured by flow cytometry using FACSCalibur™ platform. Data were analyzed by FlowJo V10 software. Results were obtained from three independent experiments.

2.4. Immunoblotting

MCF-7/KCR cells (2 × 10^6cells/well) were treated with 20 μM **10 g** for 24 h. Then cell extracts were prepared using RIPA lysis buffer (50 mM Tris (pH:7.4), 150 mM NaCl, 1 mM EDTA, 1% Triton X-100 and 1xProtease Inhibitor Cocktail), centrifuged at 13,000 rpm then supernatants were collected. The protein concentration of the supernatants was assessed by the Bradford method. 25 μg protein from the lysates were resolved on 10% SDS-PAGE and transferred to nitrocellulose membrane (Amersham). Membranes were blocked with 5% non-fat dry milk in TBST (20 mM Tris, 150 mM NaCl and 0.05% Tween20) and incubated overnight with primary MDR1 antibody (Santa Cruz sc-55,510, used in 1:500 dilution), Bip (CST #3177T, used in 1:1000 dilution) and CHOP (CST #2895T, used in 1:1000 dilution) diluted in TBST containing 1% non-fat dry milk, then with HRP-conjugated secondary antibody (DAKO). Equal loading was verified by detecting tubulin, using an anti-tubulin primary antibody (eBioscience 14–4502–82, used in 1:1000 dilution) and HRP-conjugated secondary antibody (DAKO). Membranes were developed with ECL reagent (Millipore) and visualized by C-DiGit Blot Scanner (LI-COR). The presented images are representative blots from three individual experiments.

2.5. Cell viability assay

Cells were seeded at 10^4/well density in 96-well plates. On the following day, cells were treated with either 20 μM of compound **10g** or **11g** for 24 h or with verapamil in 40 μM concentration for 2 h. To detect the sensitizing capability of compound **10g** on multidrug-resistant MCF-7/KCR cells to doxorubicin-induced toxicity, cells were treated with 20 μM of compound **10g** in combination with doxorubicin in 10; 20; 40; 50 and 60 μM concentration. Following treatments cells were washed and incubated with RPMI-1640 medium containing 0.5 mg/mL MTT reagent (Sigma-Aldrich). Formazan crystals were solubilized in DMSO and absorbance was measured at 570 nm using a Synergy HTX microplate reader (BIOTEK®). Measurements were repeated three times using 4 independent biological replicates. Absorbance values of the untreated control samples were considered as 100% viability.

2.6. Apoptosis detection

Cells were seeded at 2 × 10^6 cells/well density in 6-well plates. On the following day, cells were treated either with compound **10g** or **11g** in 20 μM concentration or with doxorubicin (5 μM) for 24 h. Combinational treatments using doxorubicin (5 μM) + verapamil (4 μM) and doxorubicin (5 μM) + **10g** (20 μM) as well as doxorubicin (5 μM) + **11g** (20 μM) were also performed. Cells were collected and stained with AnnexinV-FITC/propidium iodide (PI) (Life Technologies) according to the manufacturer's recommendation. Since fluorescent properties of PI are similar to doxorubicin, we did not show PI filters in the dot plots during analysis. Fluorescence intensities of at least 10,000 cells/sample were measured by FACSCalibur™ and data were analyzed by FlowJo V10 software. Fluorescence of Annexin V-FITC and forward scatter (FSC) were represented. Experiments were repeated three times using at least three replicates.

2.7. Molecular docking assay

Homology model of the human MDR1 was obtained from the SWISS-MODEL Repository (P08183) (Bienert et al., 2016). The three-dimensional structure of **10g** and **11g** were built manually and energy minimized using Chem3D Pro-ver 12.0. Molecular dockings were performed with AutoDock ver. 4.2.6 (Morris et al., 2010). To cover the putative ATP binding site of the receptor the grid volume was set up to 80 × 80 × 80 Å with 0.375 Å spacing and centered to the nucleotide-binding domain 2. Rotatable bonds of **10g** and **11g** as well as receptor amino acid side chains in contact with ATP were kept flexible (Kadioglu et al., 2016; Mares-Sámano et al., 2009b). Blind docking was carried out using the Lamarckian Genetic Algorithm, and 1000 dockings were done. The resultant docked complexes were ranked according to the corresponding binding free energies and inspected with AutoDock Tools ver. 1.5.6 graphical interface. The lowest energy complex in which **10g** and **11g** formed interactions with amino acids in the putative ATP binding site was selected and images were generated using Pymol ver. 2.3.4 (PyMOL Molecular Graphics System, Schrödinger, LLC.).

2.8. PharmMapper target prediction

PharmMapper is a web server that predicts therapeutic drug targets for small molecules provided as query. 2D structures of **10g** and **11g** were drawn using PubChem sketcher (“PubChem Sketcher V2.4,”). The downloaded structures were given as an input for PharmMapper available at http://www.lilab-ecust.cn/pharmmapper/. For human targets parametric value was set to 2241, maximum number of matched targets was set to 100 and all other parameters were set to default values.

2.9. JC-1 staining

To measure changes in the mitochondrial membrane potential after treatments, JC-1 staining was performed. Cells were seeded onto coverslips placed into 24-well plates (10^5 cells/well). On the following day, cells were treated with compound **10g** or **11g** in 20 μM concentration or with carbachol in 500 μM concentration for 24 h. Carbachol was used as a positive control, as it induces mitochondrial damage by raising cytoplasmic calcium levels. Since JC-1 is a MDR1 substrate, therefore, before JC-1 loading, 40 μM of verapamil was added to the samples for 1 h. Then cells were washed and incubated with RPMI-1640 medium containing 10 μg/mL JC-1 (Life Technologies) for 15 min. Coverslips were inversely mounted in Fluoromount™ (ThermoFisher) on glass slides and JC-1 fluorescence was visualized by OLYMPUS BX51 microscope equipped with an Olympus DP70 camera using the same exposition time for all samples. Image analysis was performed by ImageJ software. We have to note that pretreatment of each sample

with verapamil was required to improve intracellular retention of JC-1, a MDR1 substrate, however, in those samples which were treated with compound **10g** inevitably more JC-1 was retained since these cells received two MDR1 inhibitors (verapamil and compound **10g**) (fig S1). As a consequence, we could not apply the usual analysis and representation of JC-1 staining (aggregate/monomer ratio), but instead, the average number of mitochondria/cell was counted in case of 100 cells in each sample and expressed as a measure of mitochondrial damage. Experiments were repeated three times using three independent biological replicates.

2.10. Reverse transcription and real-time PCR

Cells were seeded at 2×10^6 cells/well density in 6-well plates. On the next day, cells were treated either with compound **10g** or **11g** in 20 μM concentration or with dithiothreitol (DTT, 2 mM) for 24 h. Total cellular RNA was prepared using RNeasy® Mini Kit (QIAGEN) according to the manufacturer's recommendation. 45 ng/μL RNA was reverse transcribed (TaqMan® Reverse Transcription kit, Applied Biosystems). PCR reactions were performed on PicoReal™ Real-time PCR (Thermo Scientific) using SYBR Green qPCR Master Mix (Thermo Scientific) with an input of 100 ng cDNA. Each primer (Table 1) was used at 200 nM concentration. Relative transcript levels were determined by the ΔΔCt analysis using GAPDH as the reference gene. Experiments were repeated three times using three biological replicates.

3. Results

3.1. Compound *10g* inhibits MDR1 efflux activity in multidrug-resistant breast cancer cells

Based on structure−cytotoxicity relationships verified previously on numerous cancer cell lines (Baji et al., 2017), compounds **10b, 10c, 10d, 10f** and **10g** and their deacetylated counterparts **11b, 11c, 11d, 11f** and **11g** (chemical structures are shown in Fig 1 and supplementary Fig S2) were selected from the compound library of synthetic heterocyclic androstane derivatives for the present investigation (the original compound numbers used in Baji et al. (Baji et al., 2017) were retained for clarity and comparability). Multidrug-resistant MCF-7/KCR cells were treated with these substances at 20 μM concentration for 24 h. Drug-resistant phenotype of MCF-7/KCR cells was confirmed previously by detecting significant MDR1 expression and high efflux activity in these cells (Gopisetty et al., 2019) and the applied concentration of the test compounds and the treatment time were established according to preliminary experiments (unpublished results). Rhodamine 123 drug efflux assay was performed to examine the potential inhibitory effects of the test compounds on MDR1 activity. The fluorescent dye Rhodamine 123 (RH123) is a substrate of MDR1, thus it can be readily expelled from drug-resistant cancer cells, whereas intracellular retention of RH123 demonstrates inhibition of MDR1. As a positive control, cells were treated with the known MDR1 inhibitor verapamil. The obtained mean intracellular RH123 fluorescence values in MCF-7/KCR cells upon treatments with the test compounds are represented in Table S1.

As expected, verapamil treatment resulted in the highest mean intracellular RH123 fluorescence (Fig 2A and Table S1). Compared to the fluorescence of cells receiving verapamil treatment (set as 100%) the lowest intracellular fluorescence was found after treating MCF-7/KCR cells with compounds **11b** (4.6%), **11d** (4.6%), **11f** (6.4%), **11g** (8.7%) and **11c** (9%), whereas the fluorescence of cells exposed to most acetylated derivatives – apart from compound **10d** (9.6%) - was significantly higher i.e. **10f** (24.6%), **10b** (30.2%), **10c** (42.6%) and **10g** (44.4%) (see Table S1). All the acetylated derivatives (**10b, 10c, 10d, 10f,** and **10g**) manifested significant inhibitory potential on MDR1 efflux activity, demonstrated by significantly higher intracellular RH123 fluorescence values, compared to the deacetylated counterparts (**11b, 11c, 11d, 11f,** and **11g**) (Fig 2A, Fig S3 and Table S1), which clearly indicates a strong structure−function relationship manifesting in multidrug-resistant MCF-7/KCR cells. Among the tested compounds, treatments with compound **10g** resulted in the highest intracellular RH123 accumulation, i.e. the strongest MDR1 inhibition (Fig 2A and Table S1). Therefore, compound **10g** was selected and applied in subsequent experiments to uncover the precise mechanisms underlying the inhibition of MDR1 efflux activity. To expose the possible differences in molecular actions between the acetylated compound (**10g**) and its deacetylated counterpart, compound **11g** (the fluorescence intensity of cells treated with **11g** was only 8.7% compared to the fluorescence of positive control) was also included in successive investigations. First, it was validated that the concentration of 20 μM of compounds **10g** and **11g** - applied in the RH123 efflux assay - would not cause significant cytotoxicity on MCF-7/KCR cells. For this, MTT assays were performed after incubating the cells for 24 h with compounds **10g** and **11g**. Results show that compared to untreated control the viable percentage of MCF-7/KCR cells treated with 20 μM of **10g** or **11g** was 77.8 ± 22.8 and 97.5 ± 19.3, respectively. This indicates that neither of these two compounds is able to induce serious cytotoxicity of drug resistant cells at 20 μM concentration (Fig 2B).

DHT is a parent compound of the selected synthesized derivatives, including **10g** and **11g**. To examine the possibility of the involvement of hormonal effects exhibited by **10g** (or by **11g**) underlying MDR1 inhibition, DHT was tested for its inhibitory activity on MDR1-mediated efflux in multidrug-resistant breast cancer cells. To achieve this, MCF-7/KCR cells were treated with 20 μM DHT for 24 h then Rhodamine 123 assay was performed. Our results indicate that DHT treatment does not lead to the inhibition of MDR1 activity (Fig 2C).

3.2. *10g* treatment sensitizes multidrug-resistant breast cancer cells to doxorubicin-induced killing

As the inhibition of MDR1 efflux leads to the intracellular retention of chemotherapy drugs, it prolongs the time for the drug to exert its anticancer activity within cancer cells, thus it improves the therapeutic efficacy. Therefore, treatment with **10g**, a MDR1 inhibitor, might sensitize multidrug-resistant MCF-7/KCR cells to doxorubicin-induced cytotoxicity. To test this hypothesis, MCF-7/KCR cells were treated with 20 μM of **10g** and with doxorubicin in 10, 20, 40, 50 and 60 μM concentrations for 24 h and compared the results with those obtained on cells receiving only doxorubicin treatment at identical concentrations as indicated above. We observed that treatment with **10g** significantly augmented the cytotoxicity provoked by doxorubicin in MCF-7/KCR cells (Fig 3A). The IC_{50} values calculated from viability curves were 55.96 ± 0.1 μM for doxorubicin and 35.26 ± 0.1 μM for **10g**+doxorubicin treatments, respectively (Fig S4). Next, we wanted to check

Table 1
Sequence of primers used in qPCR experiments.

Primer	Forward	Reverse
BIP	5′-TGTTCAACCAATTATCAGCAAACTC-3′	5′-TTCTGCTGTATCCTCTTCACCAGT-3′
CHOP	5′-GGAGCATCAGTCCCCCACTT-3′	5′-TGTGGGATTGAGGGTCACATC-3′
MDR1	5′-CTGTGATTGCATTTGGAGGA-3′	5′-CCAGAAGGCCAGAGCATAAG-3′
GAPDH	5′-TGCACCACCAACTGCTTAGC-3′	5′-GGCATGGACTGTGGTCATGAG-3′

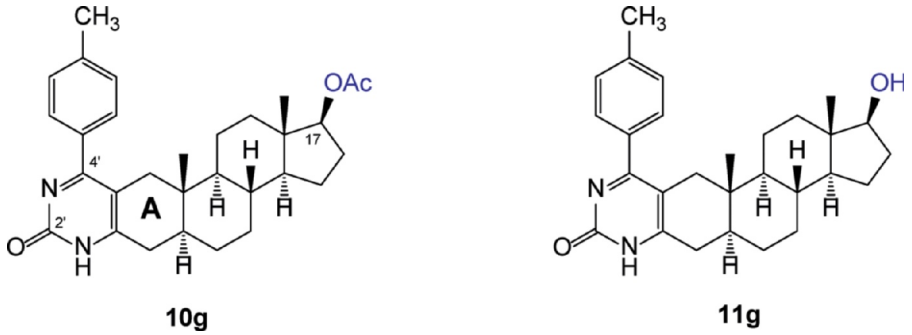

Fig. 1. Chemical structures of DHT-derived A-ring-fused pyrimidinones **10g** and **11g** differing in their C-17 functionality.

whether the improved toxic effects of doxorubicin in the presence of compound **10 g** are the result of enhanced apoptosis induction. MCF-7/KCR cells were again treated with either 20 μM of **10 g** or 5 μM doxorubicin or with the combination of 20 μM **10 g** and 5 μM doxorubicin for 24 h. Cells receiving only DMSO were considered as negative control and those treated with 4 μM verapamil for 24 h were set as positive control. The percentage of apoptotic cells (Q2 + Q3) was 0.97% in control samples, and it was 0.59% in doxorubicin-treated samples. When cells were exposed to compound **10 g** 1.86% of cells, by doxorubicin + verapamil-treated cells 26.55%, and finally, 43.22% of ***10 g*** + doxorubicin-exposed cells were undergoing apoptosis (Fig 3B). In line with the viability results, Annexin V/PI apoptosis assay clearly showed that treatments with compound ***10 g*** + doxorubicin resulted in a significantly higher number of apoptotic cells compared to cells receiving only doxorubicin treatment (Fig 3B). Surprisingly, the drug sensitizing effect of **10 g** seems to be stronger than that of verapamil, a well-known MDR1 inhibitor. As expected, treatments with 20 μM of **11 g** alone or in combination with 5 μM doxorubicin did not influence

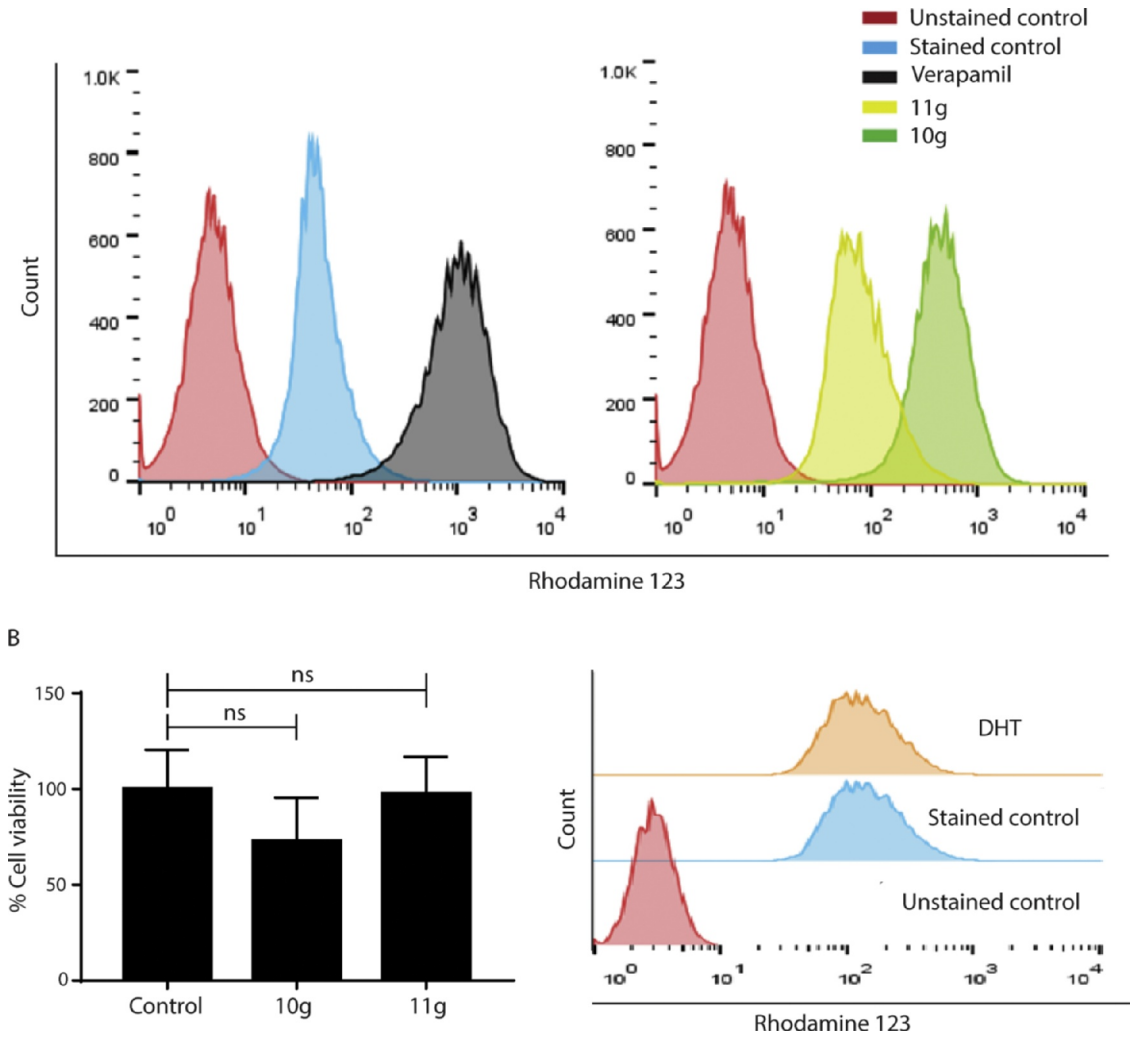

Fig. 2. Compound 10g inhibits MDR1 efflux activity. A. MCF-7/KCR cells treated with **10g** retain more intracellular Rhodamine 123, indicating inhibition of MDR1 efflux activity, whereas, treatment with **11g** did not influence the intracellular Rhodamine 123 levels compared to untreated control. B. MCF-7/KCR cells treated with 20 μM of either **10g** or **11g** for 24 h manifest no significant cytotoxicity compared to untreated control cells. C. DHT treatment did not inhibit MDR1 efflux activity in MCF-7/KCR cells.

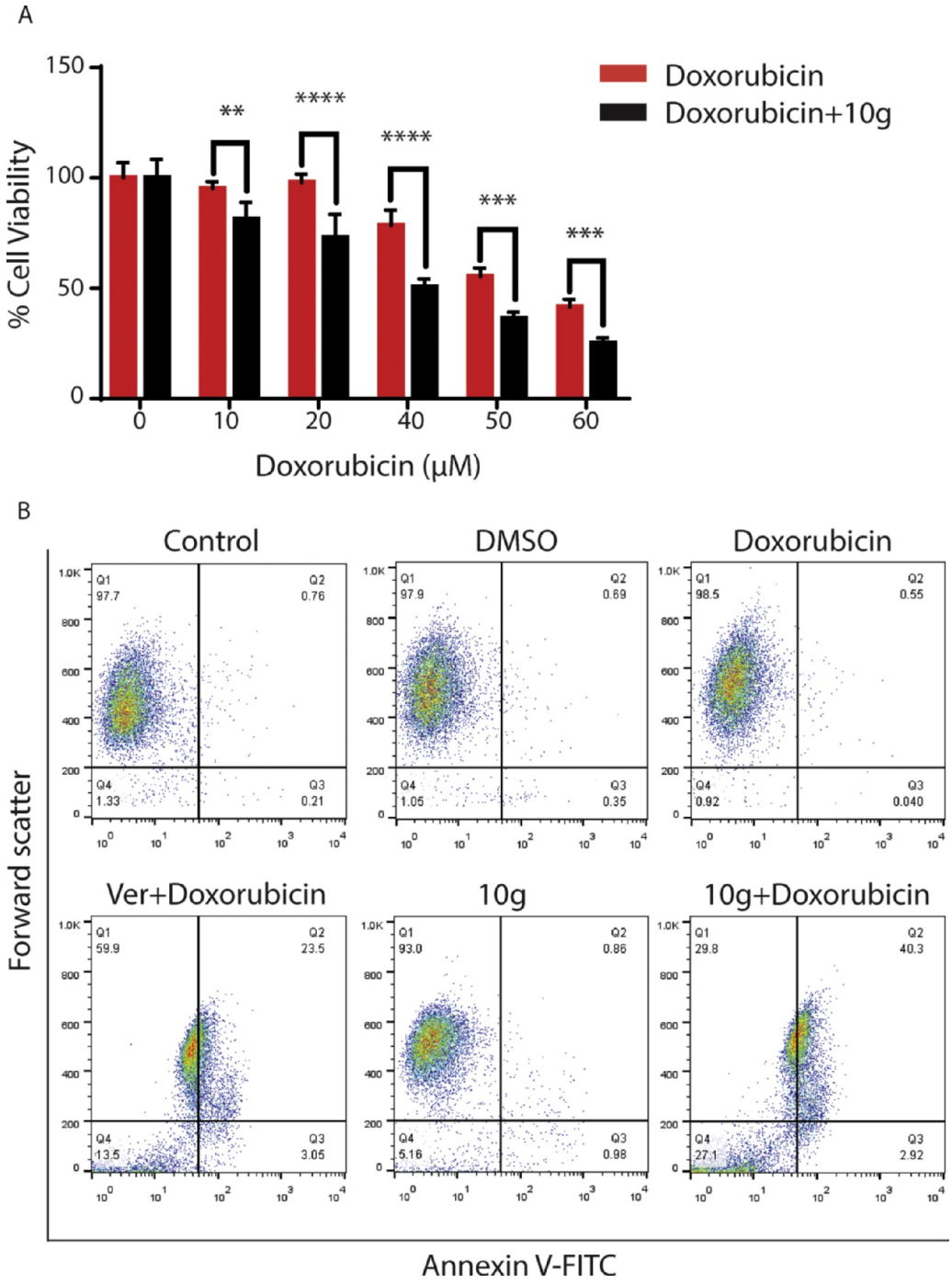

Fig. 3. Treatment of multidrug-resistant MCF-7/KCR cells with 10g sensitizes them to doxorubicin-induced apoptosis. A. Combinational treatment using doxorubicin in different concentrations and compound **10g** significantly increased cytotoxicity of MCF-7/KCR cells, assessed by MTT assay. B. Combinational treatment of doxorubicin and **10g** significantly increased the percentage of Annexin V-positive (Q2 + Q3) apoptotic cells compared to MCF-7/KCR cells receiving doxorubicin or compound **10g** alone.

MCF-7/KCR sensitivity to doxorubicin-induced apoptosis (Fig S5). These results verify the MDR1 inhibiting feature of molecule **10 g** and indicate that in fact, there is a link between MDR1 inhibition and improved doxorubicin sensitivity upon **10 g** treatment.

*3.3. In silico approaches predicted different binding targets of **10g** and **11g** but similar binding to MDR1*

Molecular docking study was carried out to predict if compound **10g** or **11g** is able to establish interactions with MDR1. In the lowest energy complex, wherein ligands were bound to the nucleotide-binding domain 2 of MDR1 (Fig 4A), the predicted binding free energy was −6,53 kcal/mol for **10g**, and −5.20 kcal/mol for **11g**, respectively. The acetoxy group of **10g** formed a hydrogen bond with Tyr^{1044} while the methyl group on the phenyl ring was predicted to interact with the side chain of Arg^{1047}. The pyrimidine ring attached with Arg^{262} and Asp^{805} side chains, while Cys^{1074} was connected to the terminal cyclopentane ring (Fig 4B). Similar binding pose was revealed in case of the deacetylated counterpart. The acetoxy substituting hydroxyl group faced to Tyr^{1044} and Arg^{1047} residues, respectively. The main difference

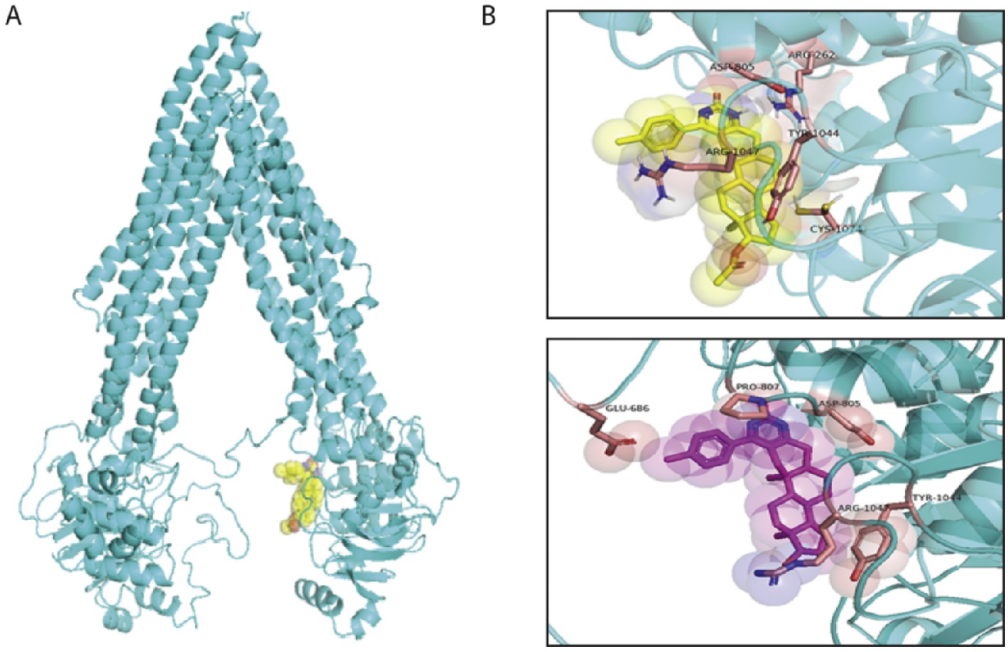

Fig. 4. ***In silico*** **molecular docking predicted the binding of 10g and 11g to MDR1**. A. Lowest energy docked complexes of **10g** and MDR1. B. Predicted interactions of **10g** and **11g** with the nucleotide-binding domain 2 of MDR1. **10g** is yellow while **11g** is magenta coloured. Receptor amino acid side chains with interactions with the ligands are labeled and pink-coloured.

Table 2
PharmMapper generated top ten druggable targets of **10g** and **11g**.

Rank	**10g** targets	**11g** targets
1	Serine/threonine-protein kinase Pim-1	Integrin alpha-L
2	Carbonic anhydrase 2	Serine/threonine-protein kinase Pim-1
3	Integrin alpha-L	Aldose reductase
4	Aldo-keto reductase C2	Aldo-keto reductase C2
5	Bone morphogenetic protein 2	Bone morphogenetic protein 2
6	Caspase-3	Caspase-7
7	Aldose reductase	PTP1B
8	Cholinesterase	Mitogen-activated protein kinase 1
9	Peptidyl-prolyl cis-trans isomerase	Kinesin-like protein KIF11
10	Mitogen-activated protein kinase 1	Aldo-keto reductase C3

in the formed interactions of **11g** that the methyl group on the phenyl ring formed interaction with the side chain of Glu^{686}. Additionally, the sterane ring interacted with Asp^{805} and Pro^{807}, respectively (Fig 4B). Since in docking studies we did not see significant differences in predicted binding properties of **10g** and **11g** to MDR1, we proceeded for PharmMapper analysis to find possible drug targets of **10g** and **11g** (Wang et al., 2017, 2016). Unlike docking studies which rely on simple free energy based fit scores, PharmMapper encompasses computational tools that use ligand-pharmacophore fit scores. Thereby, predicts *in silico* druggable targets of a query compound from annotated pharmacophore model database through reversed pharmacophore matching thus improves prediction reliability. Among the top 10 potential proteins predicted to be druggable targets of **10g** and **11g** in humans, (Table 2) carbonic anhydrase 2, caspase 3, cholinesterase and peptidyl-prolyl *cis-trans* isomerase were identified as typical **10g** targets, whereas caspase 7, PTP1B, KIF11 and aldo-keto reductase C3 were found as potential **11g** targets. However, here it has to be emphasized that both molecular docking studies and PharmMapper analysis are *in silico* tools to predict with fair confidence the molecular targets of a given compound, but are not by themselves sufficient to either support the supposed molecular mechanism or accurately prove the exact real-life targets of the compounds.

*3.4. Treatment with **10g** does not influence either transcriptionally or translationally the expression of MDR1 gene*

After we did not detect significant difference in the predicted binding properties of **10g** and **11g** to MDR1, although the MDR1-inhibiting property of compound **10g** but not of **11g** was identified, we aimed to delineate the possible molecular mechanism/s behind the **10g**-induced cellular phenomena. Inhibition of *MDR1* expression either transcriptionally and (or) translationally upon **10g** treatment can be a possible reason for the modulation of MDR1 efflux activity. It was also previously suggested that proto-oncogenes *CYCD* and *c-MYC* are able to regulate *MDR1* expression (He et al., 2000; Wang et al., 2012). Therefore, relative mRNA levels of *MDR1, CYCD* and *c-MYC* in MCF-7/KCR cells exposed to 20 μM of **10g** for 24 h were examined by quantitative real-time PCR. Our results indicate that treatments with **10g** did not change the transcript levels of either *MDR1, CYCD* or *c-MYC* suggesting that compound **10g** does not influence the mRNA expression of *MDR1* (Fig 5A). In a control experiment, the effect of compound **11g** on the expression levels of these genes was also investigated and no changes were observed compared to untreated control cells (Fig S6). Then we analyzed MDR1 protein levels of **10g**-exposed multidrug-resistant cells. Western blots revealed no difference in MDR1 protein expression between control and **10g**-treated cells (Fig 5B). Our results imply that compound **10g** is not triggering the transcriptional and translational activity of *MDR1* gene, therefore the observed inhibition of MDR1-related efflux activity upon **10g** treatment is not associated with the regulation of its expression.

*3.5. Treatments with **11g** but not with **10g** induce mitochondrial damage*

MDR1 efflux is an energy-dependent process, therefore, cellular energy status can have a direct impact on MDR1 activity. Hence, we hypothesized that if compound **10g** damages mitochondria this would attenuate the ATP-driven MDR1-mediated membrane transport. To test this hypothesis, MCF-7/KCR cells were treated with 20 μM of **10g**, and for comparison also with compound **11g** for 24 h. As a positive control, cells were exposed to 500 μM carbachol for 24 h, since carbachol induces mitochondrial damage by raising cytoplasmic calcium levels. After the treatments, JC-1 staining was performed and the stained cells were observed under fluorescence microscope. The average number of mitochondria/cell was counted and expressed as a measure of

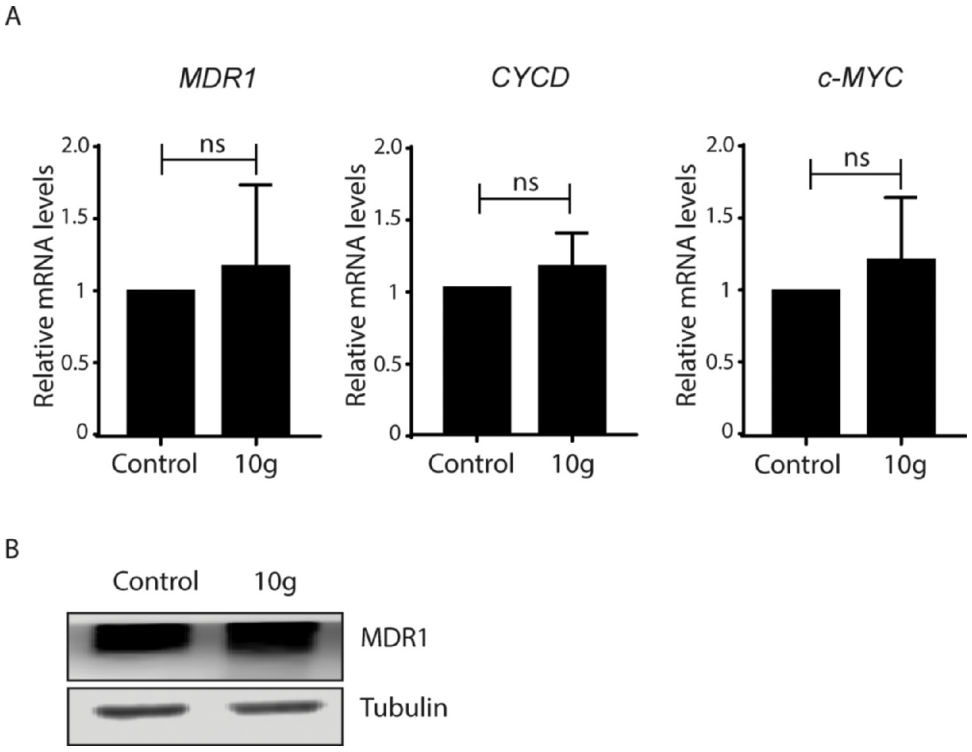

Fig. 5. 10g treatment does not affect MDR1 expression in MCF-7/KCR cells. A. Treatments with **10g** do not induce significant changes in the transcript levels of *MDR1, CYCD* and *c-MYC*. B. **10g** treatment does not affect MDR1 protein levels. Values represent mean ± SD calculated from three independent experiments.

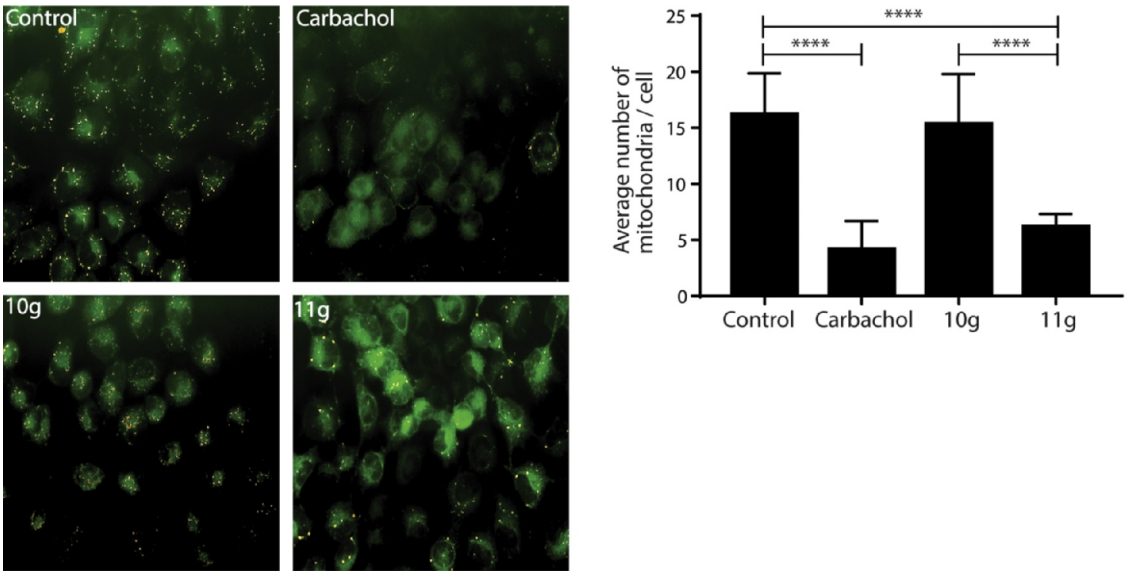

Fig. 6. 10g induced MDR1 inhibition in MCF-7/KCR cells is not the result of mitochondrial damage. In contrast to exposures of MCF-7/KCR to **10g**, where no mitochondrial damage is observed, treatment with **11g** induces significant loss of functional mitochondria (yellow colored spots in the fluorescent images). Carbachol was used as positive control. Values represent average number of mitochondria counted from at least 25 cells (****$P < 0.0001$, Fisher's LSD test).

mitochondrial damage, where lower values indicate significant damage to this organelle. Results indicate that **10g** treatment did not induce mitochondrial damage, whereas compound **11g** triggered significant reduction in the number of functional mitochondria (Fig 6). If the underlying cause of the observed inhibition of MDR1 efflux activity was the damage to mitochondria, then compound **11g** should have manifested a more efficient efflux inhibition compared to **10g**. Since this was not the case, our results rule out the direct link between **10g**-induced MDR1 inhibition and mitochondrial damage.

*3.6. Compound **10g** induces endoplasmic reticulum stress in multidrug-resistant cancer cells*

Cellular distribution of MDR1 can be disturbed due to endoplasmic reticulum (ER) stress (Gopisetty et al., 2019). Moreover, our *in silico* experiments revealed that one among the predicted druggable targets of compound **10g** is peptidyl-prolyl *cis-trans* isomerase (Table 2), which protein is strongly associated with protein folding in the ER and its inhibition leads to ER stress (Kim et al., 2008). Therefore, we supposed that if compound **10g** induces ER stress in multidrug-resistant MCF-7/

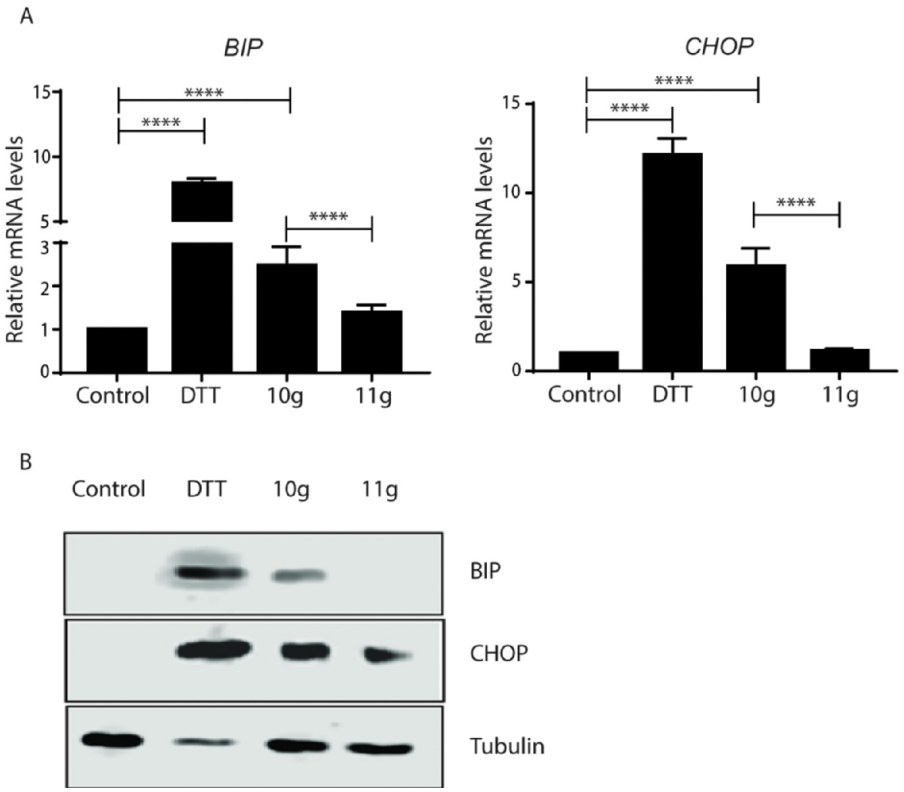

Fig. 7. 10g treatment induces endoplasmic reticulum stress in MCF-7/KCR cells. A. Treatment with compound **10g** leads to elevated relative mRNA (A) and protein (B) levels of the important ER stress response genes *BIP* and *CHOP*, as representative blots indicate. Values represent mean ± SD calculated from three independent experiments. (****$P < 0.0001$, Fisher's LSD test).

KCR cells then this could explain the attenuated MDR1 efflux activity upon treatments with **10g**. To address this issue, MCF-7/KCR cells were treated with 20 μM of **10g**, or for comparison with **11g** for 24 h and transcriptional and translational activation of ER stress response genes *BIP* and *CHOP* were measured using quantitative real-time PCR and western blot respectively. Cells exposed to 4 mM of dithiothreitol (DTT) for 24 h served as positive control for the induction of ER stress. Our results revealed that **10g** but not **11g** induces significant increase in the expression levels of the ER stress response genes *BIP* and CHOP compared to untreated control (Fig 7A, B), which implies the involvement of this cellular stress condition in the complex molecular mechanism behind MDR1 inhibition.

4. Discussion

The success of cancer chemotherapy is largely limited by inherent or attained multidrug resistance of cancer cells. Often, upon exposure to therapeutic drugs, cancer cells undergo an evolution by rewiring their molecular mechanisms resulting in cancer cell phenotypes which are capable to evade the toxic effects of therapeutic drugs. Among the various mechanisms involved in this process, the upregulation of *MDR1* is predominant since it ensures cancer cell resistance to many structurally and functionally dissimilar drugs. Fueled by ATP hydrolysis, MDR1 pumps drugs out of cancer cells keeping the intracellular amount of these agents below the required concentration to elicit cytotoxicity. Therefore, inhibition of MDR1 has always been regarded as a promising approach to improve cancer chemotherapy also in clinical settings. Despite the fact that numerous MDR1 inhibitors were tested and have failed in clinical trials due to questionable safety and thus were dismissed for further therapeutic applications, the quest for potent MDR1 modulators is still on (Chung et al., 2016).

In the present work we examined a series of pyrimidinones fused to the A-ring of DHT or DHT-acetate (Baji et al., 2017) and compared their MDR1 inhibiting properties in MCF-7/KCR cells that overexpress MDR1. Here we show a remarkable structure-related discriminative behavior manifested by these androstane-derivatives on MDR1 activity, since all the 17-acetylated derivatives **10b, 10c, 10d, 10f, 10g** exhibited a marked MDR1 inhibitory potential in contrast to their 17-OH pairs **11b, 11c, 11d, 11f, 11g** (Fig S3, Fig 2A). As compound **10g** showed the highest capacity in hindering the MDR1 efflux activity (table S1) from all the tested derivatives **10g** and its deacetylated pair **11g** were selected for subsequent experiments to unravel the possible mechanisms behind the **10g**-induced reduction in MDR1 function. Based on previous cytotoxicity tests **10g** or **11g** were applied in 20 μM concentration in further experiments as this concentration did not cause any cytotoxicity on the examined cell lines (Fig 2B). The fact that DHT, a parent compound with a similar structural platform, did not show MDR1 inhibitory activity (Fig 2C) indicates a modification-dependent gain-of-function of the acetoxy group carrying by the A-ring fused arylpyrimidinone-androstanes.

The drug resistance displayed by MCF-7/KCR signifies that such cancer cells can evade the toxic effects of unusually high concentrations of doxorubicin (Gopisetty et al., 2019). Treatment with **10g** improved cytotoxicity of doxorubicin (Fig 3A) indicated by decreased IC_{50} values for this drug (Fig S4) in cells co-treated with **10g,** compared to cells treated with doxorubicin alone. Furthermore, we proved that **10g** treatment sensitizes drug-resistant MCF-7/KCR cells to doxorubicin-induced apoptosis (Fig 3B). Surprisingly, the doxorubicin-sensitizing effect of **10g** exceeded that of the well-known, first generation MDR1 inhibitor and our positive control verapamil (Fig 3B). Molecular docking for **10g** and **11g** performed to predict their binding to MDR1 and other druggable targets, revealed no significant differences in their binding properties with MDR1 (Fig 4A, B). Nevertheless, other *in silico* approaches (such as PharmMapper) revealed different predicted binding targets for these molecules, among them peptidyl-prolyl *cis-trans* isomerase as a potential target of compound **10g**, which is a protein involved in physiological ER functions (table 2).

Down-regulation of *MDR1* expression would undoubtedly impact the quantity of drugs expelled by MDR1 efflux; therefore, we analyzed the transcript and the protein levels of MDR1 as well as the relative mRNA amount of well-known *MDR1* gene expression regulators *c-MYC* and *CYCD* following treatment of MCF-7/KCR cells with compound

10g. The results imply that these two latter genes were not transcriptionally elevated (Fig 5A) upon **10g** treatment and obeying these data *MDR1* was also not down- or upregulated either transcriptionally (Fig 5A) or translationally (Fig 5B).

Drug efflux through MDR1 is an energy-dependent process, which consumes energy from ATP hydrolysis; therefore, mitochondria - the major generators of cellular ATP - are indirectly linked to ABC transporter activity. Mitochondrial damage can lead to a reduced MDR1 efflux due to insufficient cellular ATP. A direct correlation between MDR1 inhibitory activity and cellular ATP diminishing capacity was verified in a recent report on the novel compound RY10–4 (Xue et al., 2014). To test the possibility of mitochondrial dysfunction, MCF-7/KCR cells were treated with either compound **10g** or **11g** or as a positive control with carbachol, and JC-1 staining was performed to measure mitochondrial health. We observed that treatment with molecule **11g** induced significant damage to mitochondria (Fig 6), whereas compound **10g** did not induce similar mitochondrial impairment. These findings rule out the possibility of mitochondrial damage being the underlying factor of the observed MDR1 inhibition following treatment with **10g**.

Endoplasmic reticulum is the major site of protein homeostasis. Perturbations in its function lead to ER stress and deregulation of the protein folding machinery. Since MDR1 is a glycoprotein, it requires proper handling by the ER to be capable to attain its functional conformation before reaching the plasma membrane. Endoplasmic reticulum stress perturbs the proper folding of this transport protein, which leads to a decreased number of functional MDR1 in the plasma membrane resulting in diminished efflux activity. Since a direct connection between endoplasmic reticulum stress and inhibition of MDR1 activity has already been demonstrated (Gopisetty et al., 2019), therefore we hypothesized that compound **10g** might induce endoplasmic reticulum stress as well, ultimately precipitating to a decreased efflux function. To test this hypothesis, the relative changes in the transcript and protein levels of ER stress markers *BIP* and *CHOP* were assessed in MCF-7/KCR cells treated either with compound **10g** or **11g** or with the ER stress inducer compound DTT. Our results strongly indicate that **10g** treatment induces significant endoplasmic reticulum stress, as both the mRNA and the protein levels of CHOP and BIP were increased upon **10g** exposures (Fig 7). We did not observe significant mRNA expression of these ER stress markers in multidrug-resistant cancer cells treated with molecule **11g** (Fig 7); nevertheless, the protein expression of CHOP was somewhat elevated following **11g** treatments (Fig 7B).

CHOP is activated during ER stress; however, ER stress is not the only source of CHOP activation. Cellular stresses other than ER stress through p38 MAPK also activate CHOP (Sano and Reed, 2013). Absence of transcriptional and translational elevation of BIP suggests that **11g**-induced CHOP activation might not be the result of ER stress. Moreover, stress induced CHOP activation is mostly post- transcriptional (Bi et al., 2005), which explains the possibility for observed elevation in protein but not in mRNA levels of CHOP in our results (Fig 7A, B). These findings demonstrate the reasonable implication of this cellular stress condition in the complex molecular mechanism leading to MDR1 inhibition. However, further studies are required to ascertain this connection.

The present study proved that novel A-ring-fused arylpyrimidine androstane derivatives exhibit MDR1-inhibiting potential in multidrug-resistant adenocarcinoma cells and we unraveled some of the possible molecular events underlying this feature. Furthermore, we also proved that the MDR1 inhibitory activity of these A-ring-fused arylpyrimidinones is strongly dependent on their acetylation status. With further studies, our present work can open a structural platform for the design and synthesis of new generation MDR1 inhibitors that can attenuate drug resistance and sensitize resistant cancer cells to clinically applied chemotherapy drugs. Apart from oncotherapeutic approaches, these molecules could also be utilized in the treatment of other pathological conditions like epilepsy (Summers et al., 2004).

Author contributions

All authors read and approved the final manuscript.

Funding

This research was supported by grants GINOP-2.3.2–15–2016–00,038 and EFOP-3.6.1–16–2016–00,008.

CRediT authorship contribution statement

Mohana Krishna Gopisetty: Conceptualization, Methodology, Investigation, Data curation, Writing - original draft. **Dóra Izabella Adamecz:** Methodology, Investigation. **Ferenc István Nagy:** Methodology, Investigation. **Ádám Baji:** Methodology, Investigation. **Vasiliki Lathira:** Methodology, Investigation, Data curation. **Márton Richárd Szabó:** Methodology, Investigation, Formal analysis, Visualization. **Renáta Gáspár:** Methodology, Investigation. **Tamás Csont:** Investigation, Formal analysis, Supervision, Funding acquisition. **Éva Frank:** Conceptualization, Resources, Data curation, Writing - original draft, Supervision, Funding acquisition. **Mónika Kiricsi:** Conceptualization, Resources, Writing - original draft, Writing - review & editing, Supervision, Funding acquisition.

Declaration of Competing Interest

None.

Acknowledgments

Financial support by the National Research, Development and Innovation Office-NKFIH through projects GINOP-2.3.2–15–2016–00038 and EFOP-3.6.1–16–2016–00008 and by the Ministry of Human Capacities of Hungary via grant 20391–3/2018/FEKUSTRAT is gratefully acknowledged. Furthermore, this work was supported by the UNKP-19–4-SZTE-14 (M.K.) and UNKP-20-5-SZTE-655 (M.K.) grants of the New National Excellence Program of the Ministry for Innovation and Technology and by the János Bolyai Research Scholarship of the Hungarian Academy of Sciences (BO/00878/19/8 for M.K.). The work of V. Lathira was supported by Erasmus+ Student Mobility Traineeship Program.

Supplementary materials

Supplementary material associated with this article can be found, in the online version, at doi:10.1016/j.ejps.2020.105587.

References

Baji, Á., Kiss, T., Wölfling, J., et al., 2017. Multicomponent access to androstano-arylpyrimidines under microwave conditions and evaluation of their anti-cancer activity in vitro. J Steroid Biochem Mol Biol. 172, 79–88.

Bi, M., Naczki, C., Koritzinsky, M., et al., 2005. ER stress-regulated translation increases tolerance to extreme hypoxia and promotes tumor growth. EMBO J. 24 (19), 3470–3481.

Bienert, S., Waterhouse, A., De Beer, T.A.P., et al., 2016. The SWISS-MODEL Repository-new features and functionality. Nucleic Acids Res. 45, 313–319.

Callaghan, R., Luk, F., Bebawy, M, 2014. Inhibition of the multidrug resistance P-glycoprotein: time for a change of strategy? Drug Metab Dispos. 42 (4), 623–631.

Chen, Z.S., Tiwari, A.K., 2011. Multidrug resistance proteins (MRPs/ABCCs) in cancer chemotherapy and genetic diseases. FEBS J. 278 (18), 3226–3245.

Choi, Y., Yu, A.-.M., 2014. ABC Transporters in Multidrug Resistance and Pharmacokinetics, and Strategies for Drug Development. Curr Pharm Des. 20 (5), 793–807.

Chung F.S., Santiago J.S., Francisco M., et al. *Disrupting P-Glycoprotein Function in Clinical Settings: what Can We Learn from the Fundamental Aspects of This Transporter?*2016;6(8):1583–1598.

Coley, H.M., 2010. Overcoming multidrug resistance in cancer: clinical studies of p-

glycoprotein inhibitors. Methods Mol Biol. 596, 341–358.
Cooray, H.C., Shahi, S., Cahn, A.P., Van Veen, H.W., Hladky, S.B., Barrand, M.A, 2006. Modulation of p-glycoprotein and breast cancer resistance protein by some prescribed corticosteroids. Eur J Pharmacol. 531 (1–3), 25–33.
Dayan, G., Jault, J.M., Baubichon-Cortay, H., et al., 1997. Binding of steroid modulators to recombinant cytosolic domain from mouse P-glycoprotein in close proximity to the ATP site. Biochemistry. 36 (49), 15208–15215.
De Ravel, M.R., Alameh, G., Melikian, M., et al., 2015. Synthesis of new steroidal inhibitors of P-glycoprotein-mediated multidrug resistance and biological evaluation on K562/R7 erythroleukemia cells. J Med Chem. 58 (4), 1832–1845.
Ekins, S., Kim, R.B., Leake, B.F., et al., 2002. Application of three-dimensional quantitative structure-activity relationships of P-glycoprotein inhibitors and substrates. Mol Pharmacol. 61 (5), 974–981.
Gillet, J.P., Gottesman, M.M., 2010. Mechanisms of multidrug resistance in cancer. Methods Mol Biol. 596, 47–76.
Gopisetty, M.K., Kovács, D., Igaz, N., et al., 2019. Endoplasmic reticulum stress: major player in size-dependent inhibition of P-glycoprotein by silver nanoparticles in multidrug-resistant breast cancer cells. J Nanobiotechnology. 17, 9.
Gore, R.P., Rajput, A.P., 2013. A review on recent progress in multicomponent reactions ofpyrimidine synthesis. Drug Invent Today. 5 (2), 148–152.
He, Y., Zhang, J., Zhang, J., Yuan, Y, 2000. The role of c-myc in regulating mdr1 gene expression in tumor cell line KB. Chin Med J (Engl). 113 (9), 848–851.
Ichikawa-Haraguchi, M., Sumizawa, T., Yoshimura, A., et al., 1993. Progesterone and its metabolites: the potent inhibitors of the transporting activity of P-glycoprotein in the adrenal gland. BBA - Gen Subj. 1158 (3), 201–208.
Kadioglu, O., Saeed, M.E.M., Valoti, M., Frosini, M., Sgaragli, G., Efferth, T, 2016. Interactions of human P-glycoprotein transport substrates and inhibitors at the drug binding domain: functional and molecular docking analyses. Biochem Pharmacol. 104, 42–51.
Kars, M.D., ÖD, Işeri, Gündüz, U., Ural, A.U., Arpaci, F., Molnár, J, 2006. Development of rational in vitro models for drug resistance in breast cancer and modulation of MDR by selected compounds. Anticancer Res. 26 (6 B), 4559–4568.
Kathawala, R.J., Gupta, P., Ashby, C.R., Chen, Z.S, 2015. The modulation of ABC transporter-mediated multidrug resistance in cancer: a review of the past decade. Drug Resist Updat. 18, 1–17.
Kaur, R., Kaur, P., Sharma, S., et al., 2014. Anti-Cancer Pyrimidines in Diverse Scaffolds: a Review of Patent Literature. Recent Pat Anticancer Drug Discov. 10 (1), 23–71.
Kim, J., Choi, T.G., Ding, Y., et al., 2008. Overexpressed cyclophilin B suppresses apoptosis associated with ROS and Ca2+ homeostasis after ER stress. J Cell Sci. 121 (21), 3636–3648.
Leonessa, F., Kim, J.-H., Ghiorghis, A., et al., 2002. C-7 Analogues of Progesterone as Potent Inhibitors of the P-Glycoprotein Efflux Pump. J Med Chem. 45 (2), 390–398.
Li, Y., Wang, Y.H., Yang, L., Zhang, S.W., Liu, C.H., Yang, S.L, 2005. Comparison of steroid substrates and inhibitors of P-glycoprotein by 3D-QSAR analysis. J Mol Struct. 733 (1–3), 111–118.
Lo, Y.L., Ho, C.T., Tsai, F.L, 2008. Inhibit multidrug resistance and induce apoptosis by using glycocholic acid and epirubicin. Eur J Pharm Sci. 35 (1–2), 52–67.
Luqmani, Y.A., 2005. Mechanisms of drug resistance in cancer chemotherapy. Med Princ Pract. 14 (1), 35–48.
Mares-Sámano, S., Badhan, R., Penny, J, 2009a. Identification of putative steroid-binding sites in human ABCB1 and ABCG2. Eur J Med Chem. 44 (9), 3601–3611.
Mares-Sámano, S., Badhan, R., Penny, J, 2009b. Identification of putative steroid-binding sites in human ABCB1 and ABCG2. Eur J Med Chem. 44 (9), 3601–3611.
Mohana Roopan, S., Sompalle, R, 2016. Synthetic chemistry of pyrimidines and fused pyrimidines: a review. Synth Commun. 46 (8), 645–672.
Morris, G.M., Huey, R., Lindstrom, W., et al., 2010. AutoDock4 and AutoDockTools4: automated Docking with Selective Receptor Flexibility. J comptational Chem. 30 (16), 2785–2791.
Robert, J., Jarry, C., 2003. Multidrug Resistance Reversal Agents. J Med Chem. 46 (23), 4805–4817.
Rocheblave, L., de Ravel, M.R., Monniot, E., et al., 2016. Deoxycholic acid derivatives as inhibitors of P-glycoprotein-mediated multidrug efflux. Steroids. 116, 5–12.
Sano, R., Reed, J.C., 2013. ER stress-induced cell death mechanisms. Biochim Biophys Acta - Mol Cell Res. 1833 (12), 3460–3470.
Summers, M.A., Moore, J.L., McAuley, J.W, 2004. Use of verapamil as a potential P-glycoprotein inhibitor in a patient with refractory epilepsy. Ann Pharmacother. 38 (10), 1631–1634.
Szakács, G., Chen, G.K., Gottesman, M.M, 2004. The molecular mysteries underlying P-glycoprotein-mediated multidrug resistance. Cancer Biol Ther. 3 (4), 382–384.
Szakács, G., Hall, M.D., Gottesman, M.M., et al., 2014. Targeting the Achilles Heel of Multidrug-Resistant Cancer by Exploiting the Fitness Cost of Resistance. Chem Rev. 114 (11), 5753–5774.
Wang, J., Wang, Q., Cui, Y., et al., 2012. Knockdown of cyclin D1 inhibits proliferation, induces apoptosis, and attenuates the invasive capacity of human glioblastoma cells. J Neurooncol. 106 (3), 473–484.
Wang, X., Pan, C., Gong, J., Liu, X., Li, H, 2016. Enhancing the Enrichment of Pharmacophore-Based Target Prediction for the Polypharmacological Profiles of Drugs. J Chem Inf Model. 56 (6), 1175–1183.
Wang, X., Shen, Y., Wang, S., et al., 2017. PharmMapper 2017 update: a web server for potential drug target identification with a comprehensive target pharmacophore database. Nucleic Acids Res. 45 (W1), W356–W360.
Xue, P., Yang, X., Liu, Y., Xiong, C., Ruan, J, 2014. A novel compound RY10-4 down-regulates P-glycoprotein expression and reverses multidrug-resistant phenotype in human breast cancer MCF-7/ADR cells. Biomed Pharmacother 68 (8), 1049–1056.